Toxicology Letters 299 (2018) 21–31

Contents lists available at ScienceDirect

Toxicology Letters

journal homepage: www.elsevier.com/locate/toxlet

Tributyltin impacts in metabolic syndrome development through disruption of angiotensin II receptor signaling pathways in white adipose tissue from adult female rats

Leandro Ceotto Freitas-Lima[a,*,1], Eduardo Merlo[a,1], Marina Campos Zicker[b], Juliana Maria Navia-Pelaez[c], Miriane de Oliveira[d], Luciano dos Santos Aggum Capettini[c], Célia Regina Nogueira[d], Adaliene Versiani Matos Ferreira[e], Sérgio Henrique Sousa Santos[f,g], Jones Bernardes Graceli[a,**]

[a] Department of Morphology, Healthy Sciences Center, Federal University of Espírito Santo, Brazil
[b] Department. of Food Science, Faculty of Pharmacy, Federal University of Minas Gerais, Brazil
[c] Department of Pharmacology, Biological Sciences Institute, Federal University of Minas Gerais, Brazil
[d] Department of Internal Medicine, Botucatu School of Medicine, University of São Paulo State, Botucatu, SP, Brazil
[e] Dept. of Basic Nursing, Nursing School, Federal University of Minas Gerais, Brazil
[f] Health Science Graduate Program, UNIMONTES, Montes Claros, MG, Brazil
[g] Institute of Agricultural Sciences, Food Engineering College, Federal University of Minas Gerais, Montes Claros, MG, Brazil

ARTICLE INFO

Keywords:
Adipocyte
Inflammation
Metabolic syndrome
RAS
Tributyltin chloride

ABSTRACT

White adipose tissue (WAT) dysfunction and obesity are a consequence of a low-grade inflammation state. These WAT irregularities could result from abnormal metabolic renin-angiotensin system (RAS) control. Recently, tributyltin (TBT) has been found to play a critical role in these metabolic irregularities. However, TBT actions on the WAT-RAS functions are not currently well understood. In this study, we assessed whether TBT exposure resulted in metabolic syndrome (MetS) development and other metabolic complications as a result of abnormal modulation of WAT-RAS pathways. TBT (100 ng/kg/day) was administered to adult female Wistar rats, and their WAT morphophysiology and adipokine profiles were assessed. We further assessed the expression of Angiotensin-II receptor proteins (AT1R and AT2R) and proteins involved in downstream pathways mediating inflammation and adipogenesis modulation. TBT-exposed rats exhibited increases in body weight and adiposity. TBT rats present dyslipidemia and insulin resistance, suggesting MetS development. TBT promoted WAT inflammatory infiltration, AT1R protein overexpression and reduced Angiotensin-(1–7) expression. These TBT WAT abnormalities are reflected by NFκB activation, with higher adipokine levels (leptin, TNF-α and IL-6) and overexpression of AKT, ERK, P38, FAS and PPARγ protein. *In vitro*, TBT exposure stimulates lipid accumulation, reduces AT2R protein expression, and increases leptin, AKT and ERK protein expression in 3T3L1 cells. These findings suggest that TBT exposure participates in MetS development *via* the improper function of WAT-RAS metabolic control.

1. Introduction

Metabolic syndrome (MetS) is a multifactorial diseasecharacterized by a combination of obesity, dyslipidemia, type 2 diabetes *mellitus*, and hypertension (Kelly et al., 2008; Rubio-ruíz et al., 2014). Obesity is the result of a modern lifestyle, genetics, and others factors (Lima et al., 2016). Recently, several studies have reported that xenobiotics, such as organotins (OTs), play an important role in these metabolic complications (Chamorro-Garcia et al., 2017).

OTs, such as tributyltin (TBT), are organometallic contaminants

* Corresponding author at: Laboratório de Endocrinologia e Toxicologia Celular, Departamento de Morfologia/CCS, Universidade Federal do Espírito Santo, Av. Marechal Campos, 1468, Prédio do básico I, sala 5, 290440-090 Vitória, ES, Brazil.
** Corresponding author at: Laboratório de Endocrinologia e Toxicologia Celular, Programa de Pós-Graduação em Ciências Fisiológicas/CCS, Universidade Federal do Espírito Santo, Av. Marechal Campos, 1468, Prédio do básico I, sala 5, 29043-090 Vitória, ES, Brazil.
E-mail addresses: lcf.lima@gmail.com (L. Ceotto Freitas-Lima), jbgraceli@gmail.com (J. Bernardes Graceli).
[1] Contribution author: LCFL and EM contributed equally to the study.

https://doi.org/10.1016/j.toxlet.2018.08.018
Received 18 April 2018; Received in revised form 22 August 2018; Accepted 28 August 2018
Available online 29 August 2018
0378-4274/

widely used in various agro-industries procedures (Grün and Blumberg, 2006). A subclass of these xenobiotics are called endocrine-disrupting chemicals (EDCs), which are defined as "an exogenous substance/mixture that alters function(s) of the endocrine system and consequently causes adverse health effects to an intact organism, and/or its progeny, or populations" (Bergman et al., 2012). Studies have reported that TBT increases susceptibility to metabolic diseases, such as obesity, and abnormal adipocyte function in *in vivo* and *in vitro* models. TBT is also known as an EDC subclass, the obesogens (Chamorro-Garcia et al., 2017). As consequence, abnormal white adipose tissue (WAT) enlargement is accompanied by adipocyte dysfunction, glucose/lipid metabolism impairment, and inflammation (Cairelli et al., 2013).

For many years, WAT was exclusively thought of as a fat deposit (Fujimoto and Parton, 2011). WAT is now known to be an important endocrine organ that modulates adipocyte function, but insulin sensitivity, the immune system and other systems by the production/release of adipokines (Rubio-ruíz et al., 2014). Furthermore, the obesogen TBT acts in WAT, impairing adipocyte morphophysiology, leading to abnormal inflammation (Bertuloso et al., 2015; Sena et al., 2017). Inflammation plays a critical role in obesity complications, such as abnormal adipogenesis and adipokine release, which play an important role in metabolic control (Pereira et al., 2012).

Numerous factors have been implicated in the modulation of WAT endocrine function. One of the recently emerging players is the renin-angiotensin system (RAS), which is part of the traditional system to control cardiovascular physiology and is a powerful modulator of the endocrine-metabolic role of WAT in mammals (Slamkova et al., 2016). All RAS components are expressed by adipocytes. For example, angiotensin II (Ang II), which is a principal active peptide of RAS, plays different metabolic adipocyte actions upon binding to Ang II type 1 and 2 receptors (AT1R and AT2R), such as adipogenesis and lipid/glucose metabolism control (De Picoli Souza et al., 2015; Forrester et al., 2018; Slamkova et al., 2016). In obesity, glucose/insulin intolerance and/or dyslipidemia activate the synthesis of RAS components and/or induce irregular responsiveness to Ang II peptides in different metabolic cells that mediate specific disorders of MetS, such as abnormal adipokine release and WAT inflammation (Bruce and de Kloet, 2017; Putnam et al., 2012). In our previous studies, TBT induces WAT inflammation and abnormal adipokine secretion, leading to improper metabolic control in mammals (Bertuloso et al., 2015; Sena et al., 2017). Since the discovery of the effect of the obesogenic TBT on WAT function, the effect of TBT on WAT-RAS signaling remains unclear to date. In the present study, we hypothesized that TBT promotes MetS development *via* WAT-RAS pathway modulation. We analyzed the key indicators of female rat WAT morphophysiology competence, including morphology, lipids profile, inflammation, adipokines profile and RAS components/downstream pathways. Identifying altered WAT functions due to TBT substantially contributes to our continuously evolving understanding of the WAT targets of EDCs.

2. Material and methods

Wistar female rats (12-week-old) were randomly divided into two groups. Control (CON, n = 10) rats were treated daily with vehicle solution (0.4% ethanol), and TBT (TBT, n = 10) rats were treated daily with TBT (100 ng/kg/day, Sigma Aldrich) for 15 days by gavage. As demonstrated in our previous studies, this dosing leads to metabolic abnormalities in female rats (Bertuloso et al., 2015; Sena et al., 2017). The TBT dose used in the current study was approximately 3-times lower than the tolerable daily intake level of 300 ng/kg for humans established by the U.S. Environmental Protection Agency (National Research Council (US) Committee to Review EPA's Toxicological Assessment of Tetrachloroethylene, 2010). The animals were obtained from the animal facilities of the Federal University of Espirito Santo, Brazil. The rats were fed a diet and water *ad libitum* and were housed in temperature-controlled rooms (22 °C) under a 12-hour light/dark cycle. All procedures complied with the standards stated in the Guide for the Care and Use of Laboratory Animals (Institute of Laboratory Animal Resources, National Academy of Sciences, Bethesda, MD, 1996) and were conducted under conditions approved by the local animal ethics committee CEUA/UFES (Protocol number no. 003/2016).

2.1. Measurements of body weight, food intake, and tissue collection

TBT leads to increases in body weight/fat tissue (Grün et al., 2006). Thus, the body weight (bw) was measured twice a week during TBT exposure. At the end of treatment, during the metaestrus-diestrus estrous phase, overnight-fasted rats were sacrificed by decapitation. Blood samples and white adipose tissue (WAT) were collected (retroperitoneal, parametrial (p) and mesenteric WAT), weighed (normalized by body weight) and immediately frozen in dry ice and stored at −80 °C for subsequent analysis. TBT impairs normal metabolic function (Bertuloso et al., 2015). Thus, glucose tolerance and insulin sensitivity tests (GTT and IST) were assessed. For the GTT, D-glucose (2 mg/g bw) was intraperitoneally (ip) injected into overnight-fasted rats. Glucose levels from tail blood samples were monitored at 0, 15, 30, 60, and 90 min. IST was performed on overnight-fed rats, after an *ip* injection of insulin (0.75 units/kg bw). Tail blood samples were obtained 0, 30, 60, 90 and 120 min after injection (Pereira et al., 2012).

2.2. Insulin and lipid profile assessment

TBT leads to abnormal insulin levels and lipids profile (Sena et al., 2017). Thus, serum insulin levels were measured in overnight-fasted rats using a radioimmunoassay according to the manufacturer's instructions (Diagnostic Prod. Corporation, LA, CA) (Bertuloso et al., 2015). Total serum cholesterol, triglycerides (TG), high-density lipoprotein cholesterol (HDL) and low-density lipoprotein cholesterol (LDL) were measured using colorimetric kits according to the manufacturer's directions (Bioclin®, MG, Brazil) (Lima et al., 2012).

2.3. Histological analyses

TBT induces WAT abnormalities (Penza et al., 2011). Thus, WAT morphology was evaluated. Parametrial WAT (pWAT) was fixed in paraformaldehyde diluted in phosphate-buffered saline (4% PF-PBS) pH 7.4 for 24–48 h at room temperature. Paraffin-embedded pWAT was sectioned into 5-μm thick slices and stained with H&E to visualize morphology. WAT diameter and the number of adipocytes were determined. Briefly, the adipose diameter was determined as the mean of distance of the major and minor adipocyte diameters, and quantification of adipocytes was performed and expressed as the number per unit area (mm^2) (Ludgero-Correia et al., 2012). All histomorphometric analyses were performed in a blinded manner and examined under a light microscope (Olympus BX43 with a camera Olympus Q-color 5).

2.4. Inflammation assessment

TBT is associated with the inflammatory process (Sena et al., 2017). Thus, WAT inflammation was evaluated by histology, biochemical, immunoblotting and ELISA assays. The presence of mast cells in the pWAT was determined using Alcian Blue according to a standard protocol (Sigma). Twenty photomicrographs (40x objective) for each section were used to analyze the number of positively stained cells. WAT areas for analysis were randomly selected, and fields containing medium-sized blood vessels were carefully avoided. The number of positively stained cells was then expressed per unit area (mm^2).

2.5. Myeloperoxidase and n-acetyl-β-d-glucosaminidase activity assessment

The extent of neutrophil and macrophage accumulation in the pWAT was measured by assaying myeloperoxidase (MPO) and *N*-acetyl-

β-D-glucosaminidase (NAG) activities (Barcelos et al., 2005). Briefly, WAT was homogenized in 0.02 mol/L $NaPO_4$ buffer (pH 4.7) and centrifuged, and the pellet was resuspended in 0.05 mol/L $NaPO_4$ buffer (pH 5.4). Suspensions were then subjected a freeze-thaw cycles, and supernatants were used for MPO assays by measuring the change in optical density (OD) at 450 nm. In the NAG assay, WAT was homogenized in 0.9% saline containing 0.1% v/v Triton X-100 and centrifuged. Supernatants were used to measure the change in optical density (OD) at 405 nm. Both results were expressed as a change in OD/mg wet tissue (Araújo et al., 2010).

2.6. Immunoblotting

PWAT was homogenized in lysis buffer, and total protein was obtained (Bertuloso et al., 2015). Briefly, the proteins were transferred to nitrocellulose membranes in Tris-glycine buffer (Bio-Rad). Membranes were incubated overnight with 5% blotting-grade blocker that contained nonfat dry milk in Tris-buffered saline plus 0.1% Tween 20 solution and specific antibodies. The following primary antibodies were used: AT1R (#sc1173, 1:500, SCBT), AT2R (#sc9040, 1:500, SCBT), Akt1 (#sc55523, 1:500, SCBT), p-Akt1 (#sc135650, 1:500, SCBT), PPARγ (#sc7273, 1:500, SCBT), ED1 (#MCA341R, 1:500, Bio-Rad), anti-leptin (#ab9749, 1:500, Abcam), Adiponectin (#2789, 1:500, Cell Signaling), p38 MAPK (#9212, 1:500, Cell Signaling), phospho-p38 MAPK (#9211, 1:500, Cell Signaling), Erk1/2 (#9102, 1:500, Cell Signaling), phospho-Erk1/2 (#9101, 1:500, Cell Signaling), NF-κB p50 (#sc166588, 1:500, SCBT), NF-κB p65 (#sc372, 1:500, SCBT), IκB-α (#sc847, 1:500, SCBT), anti-β-actin (sc-130657, 1:1000; SCBT, Inc) and anti-GAPDH (#sc25778, 1:1000, SCBT). Goat anti-rabbit IgG-alkaline phosphatase conjugate (A3687, 1:1000, Sigma Aldrich) was used as a secondary antibody for all blotting assays unless noted. The blots for all proteins of interest and respective GAPDH controls were visualized using a color development reaction that contained nitroblue tetrazolium chloride and 5-bromo-4-chloro-3-indolylphosphate p-toluidine salt (sc24981, SCBT). All proteins of interest and GAPDH bands were analyzed by densitometry using ImageJ software. The relative expression levels were normalized by dividing the values for the protein of interest by the corresponding internal control values.

2.7. Cytokines assays

PWAT was homogenized in extraction buffer (100 mg of tissue per 1 mL) containing 0.4 M NaCl, 0.05% Tween 20, 0.5% BSA, 0.1 mM phenylmethyl sulfonyl fluoride (PMSF), 0.1 mM benzethoniumchloride, 10 mM EDTA and 20 KI aprotinin using Ultra-Turrax. The suspension was then spun at 10,000 g for 10 min at 4 °C. The supernatant was used for ELISA assays, which were performed using kits from R&D Systems (Minneapolis, MN, USA) for murine TNF-α, IL-4, IL-6, IL-10 and IL-13 according to the manufacturer's instructions. All samples were assayed in duplicate. The threshold of sensitivity for each cytokine/chemokine was 7.5 pg/mL (Canesso et al., 2014).

2.8. Immunohistochemistry

Immunohistochemistry was performed with paraffin-embedded sections (5 μm) of pWAT. Ang-(1–7) peptide was stained using rabbit polyclonal anti-Ang-(1–7) antibody (1:950; Peninsula Laboratory, CA, USA) followed by a secondary antibody conjugated with biotin. Immunopositive signals were detected with streptavidin HRP (K069089, Universal LSAB™, for DAKO autostainer), visualized with DAB (Vector Laboratory, Burlingame, CA, USA), and counterstained with hematoxylin. Nonspecific binding was controlled by substituting a negative control for the primary antibody. Images were obtained *via* light microscopy (Endlich et al., 2017).

2.9. T3-L1 cell culture

TBT promotes adipogenesis *in vitro* models (Grün et al., 2006). Thus, we evaluated the obesogenic TBT effect *in vitro* using the 3T3-L1 cell line (Bertuloso et al., 2015). After cells grew to confluence, the differentiation process was initiated by culture for 3 days in DMEM containing 10% FBS, 0.5 mM 1-methyl-3-isobutylxanthine (IBMX) (Sigma), 1 μM dexamethasone, and 1 μg/ml insulin (Sigma). After this period, cells were maintained for 10 days in DMEM containing 10% FBS and 1 μg/ml insulin. Following the cell differentiation period, adipocytes were subjected to hormone depletion for 24 h in DMEM supplemented with charcoal-stripped fetal serum. Subsequently, cells were treated with TBT (10 nM) for 24 h, and the untreated group was considered the control group (CON).

2.10. Oil red O staining of 3T3-L1 cells

After 10 days of differentiation, cells were washed with PBS, fixed with 37% formaldehyde, and then washed again with PBS. After fixation, the cells were stained for 2 h with Oil Red O solution and then washed with distilled water (Sigma). Cell differentiation was evaluated by the presence of lipid droplets stained with Oil Red O. Fifteen random fields from each well were photographed under phase contrast microscopy and analyzed using ImageJ. The images were converted into high-contrast black and white images (to visualize the lipid droplets) and scored as the percentage area per field.

2.11. Immunoblotting of 3T3-L1 cells

After treatment, the 3T3-L1 cells were harvested and lysed. Total protein content was determined (Bertuloso et al., 2015). Briefly, all the extracts were solubilized, and SDS-PAGE and immunoblotting were performed as described above for AT1R, AT2R, Akt1, p-Akt1, anti-leptin, adiponectin, Erk1/2, phospho-Erk1/2 and GAPDH proteins.

2.12. Statistical analysis

Analyses were performed using GraphPad Prism 5.3 software. The normality of the data (Kolmogorov–Smirnov test with Lilliefors' correction) was tested. The results are presented as the mean ± SEM. Comparisons between two groups were performed using Student t-test. Two-way ANOVA was used for graph lines to verify the interaction between the independent variables (time and strain) and followed by Bonferroni posttest. A $p < 0.05$ was considered significant.

3. Results

3.1. TBT increased body weight and adiposity

TBT effects on body weight and adiposity were measured (Fig. 1). TBT rats presented increased body weight compared with the CON rats (CON: 223.00 ± 1.62; TBT: 235.68 ± 2.02 g, $n = 10$, $p < 0.05$, Fig. 1A). As expected, the area under curve (AUC) for body weight was increased in TBT rats ($p < 0.05$, Supplemental Fig. 1A). TBT rats exhibited increased adiposity compared with CON rats (CON: 0.03 ± 0.001; TBT: 0.04 ± 0.002 g/g, $n = 10$, $p < 0.05$, Fig. 1B). As predicted, increased retroperitoneal and parametrial WAT (pWAT) weights were observed in TBT rats ($p < 0.05$, Supplemental Fig. 1B and C). However, no difference in the mesenteric WAT weight was noted between CON and TBT rats ($p > 0.05$, Supplemental Fig. 1D).

3.2. TBT impaired glucose metabolism

Basal serum glucose levels, glucose tolerance and insulin sensitivity tests (GTT and IST) and serum insulin levels assessments were performed (Fig. 1). No significant changes were observed in basal serum

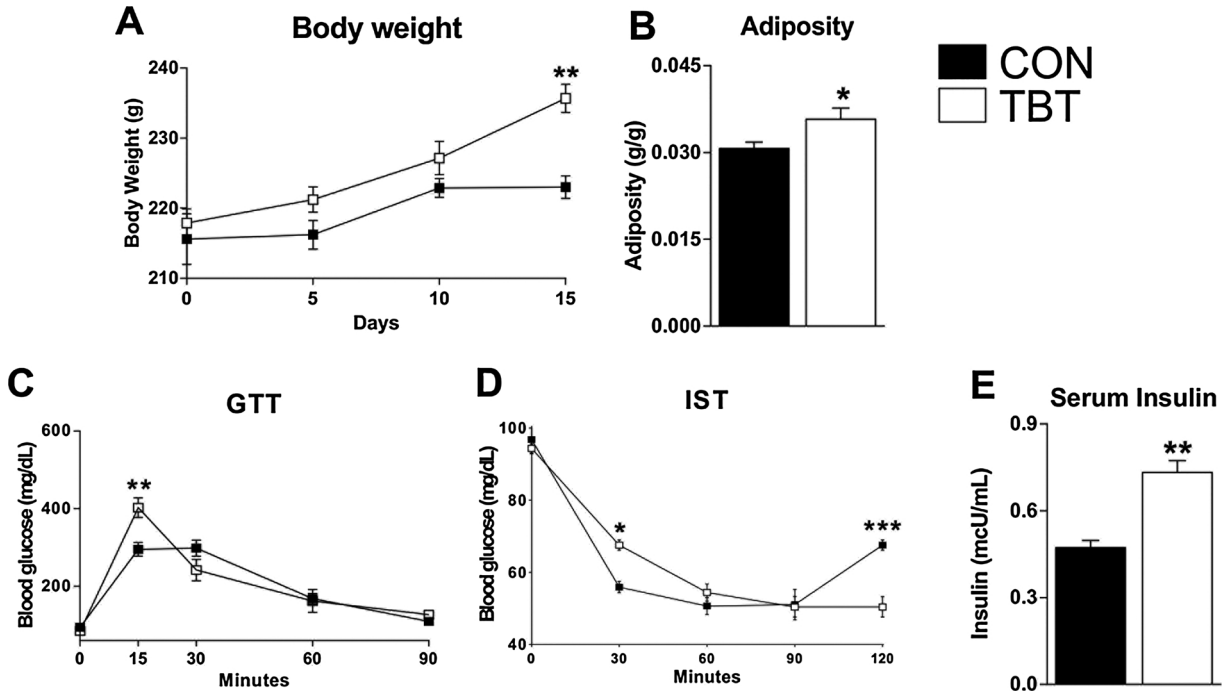

Fig. 1. TBT exposure leads to obesity and insulin resistance in female rats. (A) The TBT rats showed an increased body weight (n = 10). (B) The increased adiposity in TBT rats (n = 10). (C–D) The altered glucose tolerance and insulin sensibility tests in TBT rats confirms the insulin resistance (n = 5). (E) Hyperinsulinemia in TBT rats (n = 5). All data is expressed as the mean ± SEM. Student's t-test. Two-way ANOVA (Bonferroni's multiple comparison test). * $p < 0.05$, ** $p < 0.01$.

glucose levels between CON and TBT rats (n = 5, $p > 0.05$). TBT rats exhibited a change in GTT at 15 min (CON: 295.00 ± 17.50; TBT: 402.67 ± 25.39 mg/dL, n = 5, $p < 0.05$, Fig. 1C) and mild insulin resistance (CON: 55.93 ± 1.54; TBT: 67.58 ± 1.42 mg/dL, n = 5, $p < 0.05$, Fig. 1D) compared with CON rats. Serum insulin levels corroborate the GTT and IST alterations in TBT rats (CON: 0.47 ± 0.02; TBT: 0.73 ± 0.04 μU/mL, n = 5, $p < 0.05$, Fig. 1E).

3.3. TBT induced dyslipidemia

Serum cholesterol, triglycerides (TG), HDL and LDL levels were analyzed (Table 1). Serum cholesterol ($p < 0.05$) and TG levels ($p < 0.05$) increased in TBT rats compared with CON rats. In addition, lower serum HDL levels ($p < 0.05$) and higher serum LDL levels were observed in TBT rats ($p < 0.05$).

3.4. TBT induced adipocyte hypertrophy

Adipocyte number and diameter were evaluated (Fig. 2). Regular adipocyte features were observed in CON rats (Fig. 2A). However, hypertrophy was observed in TBT adipocytes, which were surrounded by inflammatory cells, compared with CON adipocytes (Fig. 2B). As expected, the adipocyte diameter increased in TBT rats compared with CON rats (CON: 0.85 ± 0.06; TBT: 1.31 ± 0.10 μm, n = 5, $p < 0.05$, Fig. 2C), whereas the adipocyte number was reduced in TBT rats compared with CON rats (CON: 1.74 ± 0.07; TBT: 1.16 ± 0.08 adipocytes/mm^2, n = 5, $p < 0.05$, Fig. 2D).

Table 1
Serum lipid profile of CON and TBT rats.

Lipid profile	Group	
	CON	TBT
Cholesterol (mg/dL)	61.4 ± 2.9	76.4 ± 4.4*
Triglycerides (mg/dL)	56.0 ± 2.6	66.0 ± 3.2*
HDL (mg/dL)	35.5 ± 3.9	23.8 ± 3.2*
LDL (mg/dL)	17.8 ± 2.3	26.5 ± 2.2*

HDL: High density lipoprotein; LDL: Low-density lipoprotein. Values are expressed as the mean ± SEM.
* $p < 0.05$ *vs.* CON (Student's t test).

3.5. TBT induced WAT inflammation

Alcian Blue staining, MPO and NAG activity, and ED1 immunoblotting were performed (Fig. 2). An increase in WAT mast cell number in TBT rats was observed (CON: 46.86 ± 3.86; TBT: 75.42 ± 5.79 mast cells/mm^2, n = 5, $p < 0.05$, Fig. 2E, F, and G). WAT MPO activity was increased in TBT rats compared with CON rats (CON: 0.13 ± 0.01; TBT: 0.21 ± 0.01 OD/mg of wet tissue, n = 5, $p < 0.05$, Fig. 2H), indirectly indicating the presence of neutrophils. Both WAT NAG activity ($p > 0.05$, Fig. 2I) and ED1 protein expression ($p > 0.05$, Fig. 2J) were similar between CON and TBT rats.

3.6. TBT activated WAT NF-κB expression

WAT NF-κB subunit protein expression was evaluated (Fig. 2K). Here, p50 (CON: 1.00 ± 0.04; TBT: 1.21 ± 0.09, n = 5, $p < 0.05$, Fig. 2K) and p65 (CON: 1.00 ± 0.13; TBT: 1.56 ± 0.16, n = 5, $p < 0.05$, Fig. 2K) subunit protein expression increased in TBT rats compared with CON rats. However, IκB subunit protein expression was reduced in TBT rats (CON: 1.00 ± 0.06; TBT: 0.77 ± 0.04, n = 5, $p < 0.05$, Fig. 2K).

3.7. TBT promoted an abnormal serum adipokine profile

To assess the TBT effects on serum adipokines levels, serum leptin and adiponectin levels were measured (Fig. 2). Serum leptin levels increased in TBT rats compared with CON rats (CON: 2.19 ± 0.39; TBT: 4.49 ± 0.68 × 10^3 pg/dL, n = 5, $p < 0.05$, Fig. 2L). A reduction in serum adiponectin levels was observed in TBT rats (CON: 2.73 ± 0.16; TBT: 2.22 ± 0.07 × 10^6 pg/ml, n = 5, $p < 0.05$, Fig. 2M).

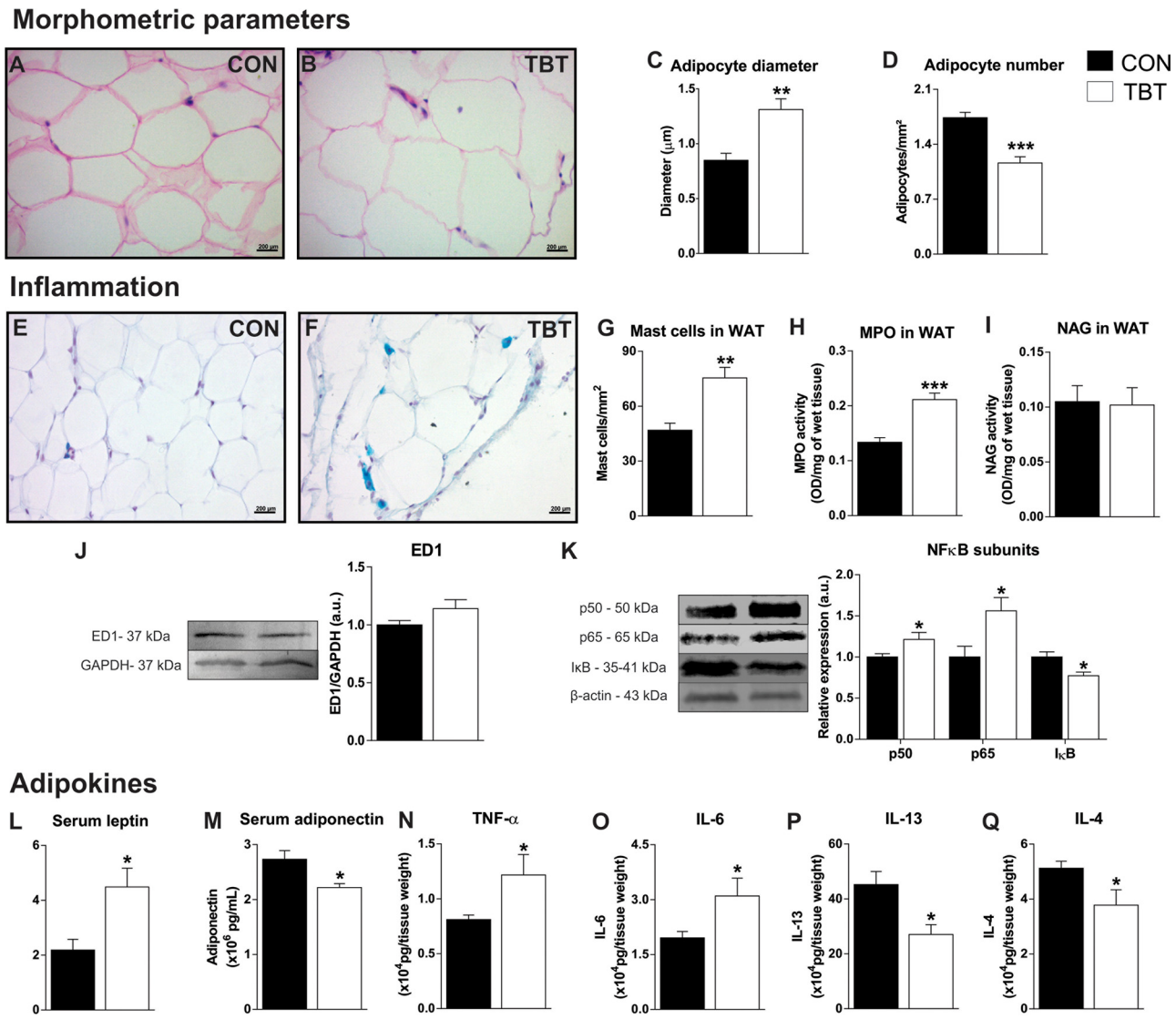

Fig. 2. TBT exposure induces WAT expansion and inflammation in female rats. (A) Photomicrography of H&E stained WAT from CON rats showing normal morphologic aspects of adipocytes. (B) Photomicrography of H&E stained WAT from TBT rats shown inflammatory cells surrounding adipocytes hypertrophic. (C) Higher WAT adipocyte diameter in TBT rats (n = 5) and (D) Lower WAT adipocyte number in TBT rats (n = 5). (E–F) Representative photomicrography of Alcian blue stained WAT from CON and TBT rats represents the (G) higher mast cells number in WAT from TBT rats (n = 5). (H) Higher MPO activity in WAT from TBT rats indirectly reflects the neutrophils presence in adipocyte (n = 5), and the (I) NAG activity in WAT from CON and TBT rats indirectly reflects the activate macrophages presence in adipocyte (n = 5). (*J*) ED1 protein expression in WAT from CON and TBT rats indicates the macrophages quantification (n = 4). (K) NFκB subunits (increased p50 and p65, reduced IκB) protein expression in WAT from TBT rats (n = 4). L–M, hyperleptinemia and hypoadiponectinemia in TBT rats (n = 5). (N–Q) Higher TNF-α, and IL-6, and lower IL-13 and IL-4 WAT levels in TBT rats (n = 5). All data is expressed as the mean ± SEM. Student's t-test. * $p < 0.05$, ** $p < 0.01$, *** $p < 0.001$. Bar = 200 μm (For interpretation of the references to colour in this figure legend, the reader is referred to the web version of this article.).

3.8. TBT impaired WAT cytokines levels

The levels of WAT cytokines, including TNF-α, IL-6, IL-13 and IL-4, were evaluated. The levels of pro-inflammatory cytokines TNF-α (CON: 0.81 ± 0.04; TBT: 1.22 ± 0.19 × 10^4pg/tissue weight, n = 5, $p < 0.05$, Fig. 2N) and IL-6 (CON: 1.96 ± 0.17; TBT: 3.10 ± 0.48 × 10^4pg/tissue weight, n = 5, $p < 0.05$, Fig. 2O) were increased in WAT-TBT rats compared with WAT-CON rats, whereas levels of the anti-inflammatory cytokines IL-13 (CON: 45.21 ± 4.77; TBT: 27.07 ± 3.54 × 10^4pg/tissue weight, n = 5, $p < 0.05$, Fig. 2P) and IL-4 (CON: 5.12 ± 0.26; TBT: 3.78 ± 0.56 × 10^4pg/tissue weight, n = 5, $p < 0.05$, Fig. 2Q) were reduced in WAT-TBT rats compared with WAT-CON rats.

3.9. TBT disrupted WAT RAS signaling in vivo

The expression of angiotensin II receptors (AT1R and AT2R), Ang (1–7) and proteins/enzymes involved in downstream pathways were evaluated (Fig. 3). In addition, pWAT AT1R protein expression was increased in TBT rats compared with CON rats (CON: 1.00 ± 0.11; TBT: 1.68 ± 0.21, n = 5, $p < 0.05$, Fig. 3A). No significant change was observed in pWAT AT2R protein expression between CON and TBT rats ($p > 0.05$, Fig. 3A). Ang (1–7) was visualized using an IHC protocol (Fig. 3B-C). In addition, pWAT Ang (1–7) is reduced in TBT rats compared with CON rats (arrowhead, Fig. 3C and B). Total pWAT AKT protein expression was increased in TBT rats (CON: 1.00 ± 0.01; TBT: 1.13 ± 0.03, n = 5, $p < 0.05$, Fig. 3D). However, the p-AKT/AKT ratio was similar between CON and TBT rats ($p > 0.05$, Fig. 3D). TBT rats exhibited an increase in total pWAT p38 protein expression (CON: 1.00 ± 0.01; TBT: 2.18 ± 0.28, n = 4, $p < 0.05$, Fig. 3E). However,

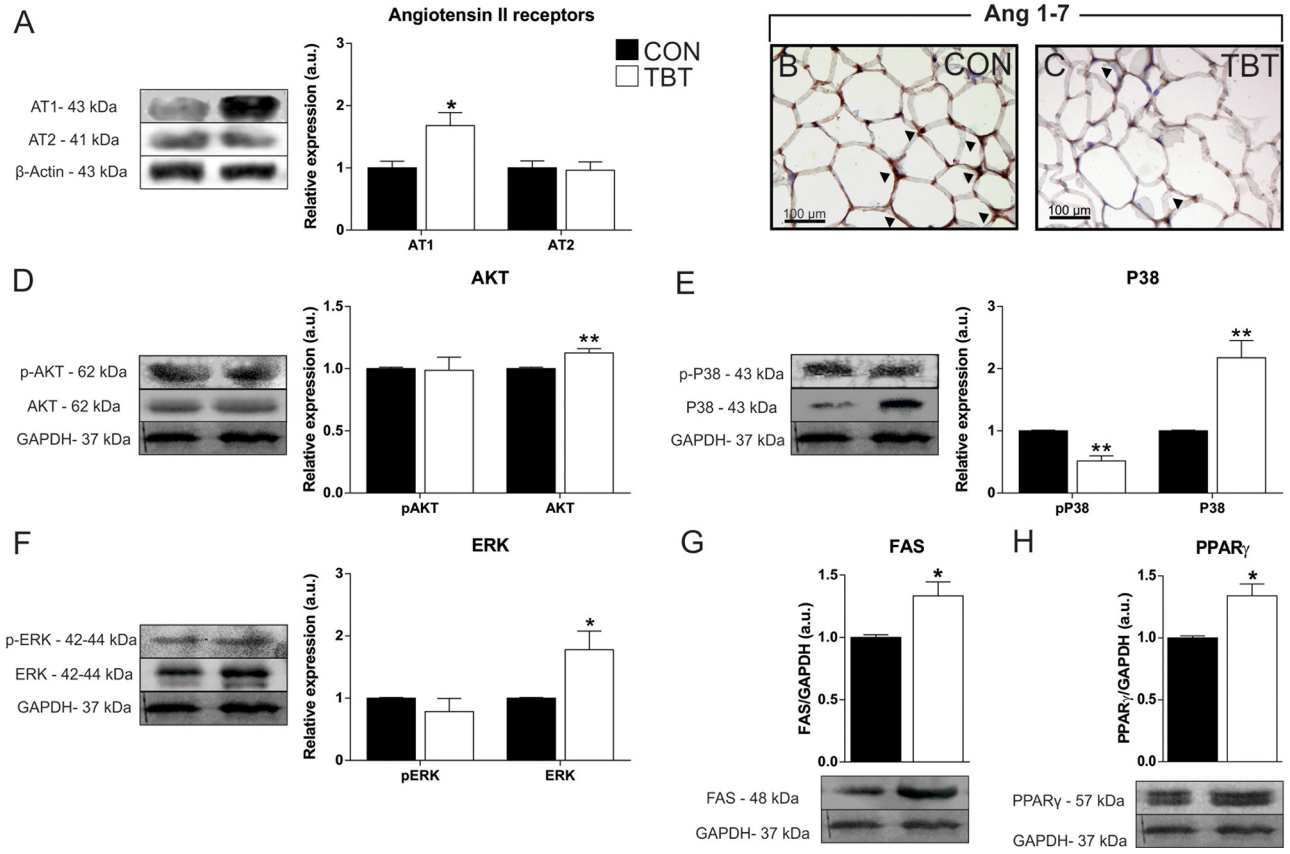

Fig. 3. TBT exposure causes WAT AT1 overexpression and RAS pathway alteration in female rats. (A) Angiotensin II receptors (AT1R and AT2R) protein expression, increased AT1R expression in TBT rats (n = 4). (B) Representative WAT Ang 1–7 IHC photomicrography of CON showing normal Ang 1–7 presence; (C) Photomicrography of Ang 1–7 IHC of WAT from TBT rats was reduced Ang 1–7 presence. Arrowhead indicates Ang 1–7. (D) p-AKT/AKT ratio and increased total AKT protein expression in WAT from TBT rats (n = 4). (E) reduced p-p38/p38 ratio and increased total p38 protein expression in WAT from TBT rats (n = 4). (F) p-ERK/ERK ratio and increased total ERK protein expression in WAT from TBT rats (n = 4). (G) Increased FAS protein expression in WAT from TBT rats (n = 4). (H) Increased PPARγ protein expression in WAT from TBT rats (n = 4). All data is expressed as the mean ± SEM. Student's t-test. * $p < 0.05$, ** $p < 0.01$. Bar = 100 µm.

the p-p38/p38 ratio is reduced in TBT rats compared with CON rats (CON: 1.00 ± 0.01; TBT: 0.52 ± 0.08, n = 4, $p < 0.05$, Fig. 3E). Total pWAT ERK protein expression increased in TBT rats (CON: 1.00 ± 0.01; TBT: 1.78 ± 0.30, n = 4, $p < 0.05$, Fig. 3F). However, the pERK/ERK ratio was similar between CON and TBT rats ($p > 0.05$, Fig. 3F). Moreover, pWAT FAS (CON: 1.00 ± 0.02; TBT: 1.34 ± 0.10, n = 4, $p < 0.05$, Fig. 3G) and PPARγ protein expression increased in TBT rats compared with CON rats (CON: 1.00 ± 0.02; TBT: 1.33 ± 0.11, n = 4, $p < 0.05$, Fig. 3H).

3.10. TBT induced abnormal lipid deposition and adipokine levels in 3T3-L1 cells

To assess TBT effects in 3T3-L1 cells, we evaluated the lipid deposition by Oil red O staining as well as adiponectin and leptin protein expression (Fig. 4). TBT increased lipid deposition in 3T3-L1 cells compared with CON cells (CON: 6.44 ± 0.38; TBT: 11.09 ± 0.64, n = 6, $p < 0.05$, Fig. 4A–C). Leptin protein expression was increased in 3T3-L1 cells exposed to TBT compared with CON cells (or vehicle cells) (CON: 1.00 ± 0.16; TBT: 1.67 ± 0.17, n = 3, $p < 0.05$, Fig. 4D) and adiponectin protein expression was reduced (CON: 1.00 ± 0.04; TBT: 0.53 ± 0.02, n = 3, $p < 0.05$, Fig. 4D).

3.11. TBT disrupted WAT RAS signaling in vitro

TBT exposure *in vitro* also altered the RAS pathway in pre-adipocytes (Fig. 4). AT1R protein expression was not significantly altered after TBT exposure in 3T3-L1 cells ($p > 0.05$, Fig. 4E). Although AT2R protein expression was reduced in 3T3-L1 cells after TBT exposure compared with CON exposure cells (vehicle) (CON: 1.00 ± 0.01; TBT: 0.90 ± 0.04, n = 3, $p < 0.05$, Fig. 4E), total AKT protein expression was similar between CON and TBT-treated cells ($p > 0.05$, Fig. 4F). Although the pAKT/AKT ratio increased in TBT-treated cells compared with CON cells (CON: 1.00 ± 0.01; TBT: 2.36 ± 0.46, n = 3, $p < 0.05$, Fig. 4F), total ERK protein expression exhibited no significant changes between TBT and CON cells (CON: 1.00 ± 0.01; TBT: 1.07 ± 0.17, n = 3, $p > 0.05$, Fig. 4G). However, the pERK/ERK ratio increased in TBT cells (CON: 1.00 ± 0.01; TBT: 1.47 ± 0.09, n = 3, $p < 0.05$, Fig. 4G).

4. Discussion

Our study demonstrates that TBT promotes metabolic syndrome (MetS) at least in part by *via* improper metabolic function of the white adipose tissue (WAT) renin-angiotensin system (RAS) in female rats. Increases in body weight/adiposity, glucose/insulin intolerance, insulin levels, and dyslipidemia were observed in TBT rats. Hypertrophic WAT was inflamed and characterized by the presence of mast cells, neutrophils and macrophages; activation of NFkB; increased TNF-α and IL-6 levels, hyperleptinemia and hypoadiponectinemia in the TBT rats. High angiotensin II (Ang II) type 1 receptor (AT1R), AKT, ERK, P38, FAS, and PPARγ protein expression and a reduction in Ang (1–7) protein expression was also observed in WAT-TBT rats. *In vitro*, increased lipid accumulation, reduced Ang II type receptor (AT2R) and

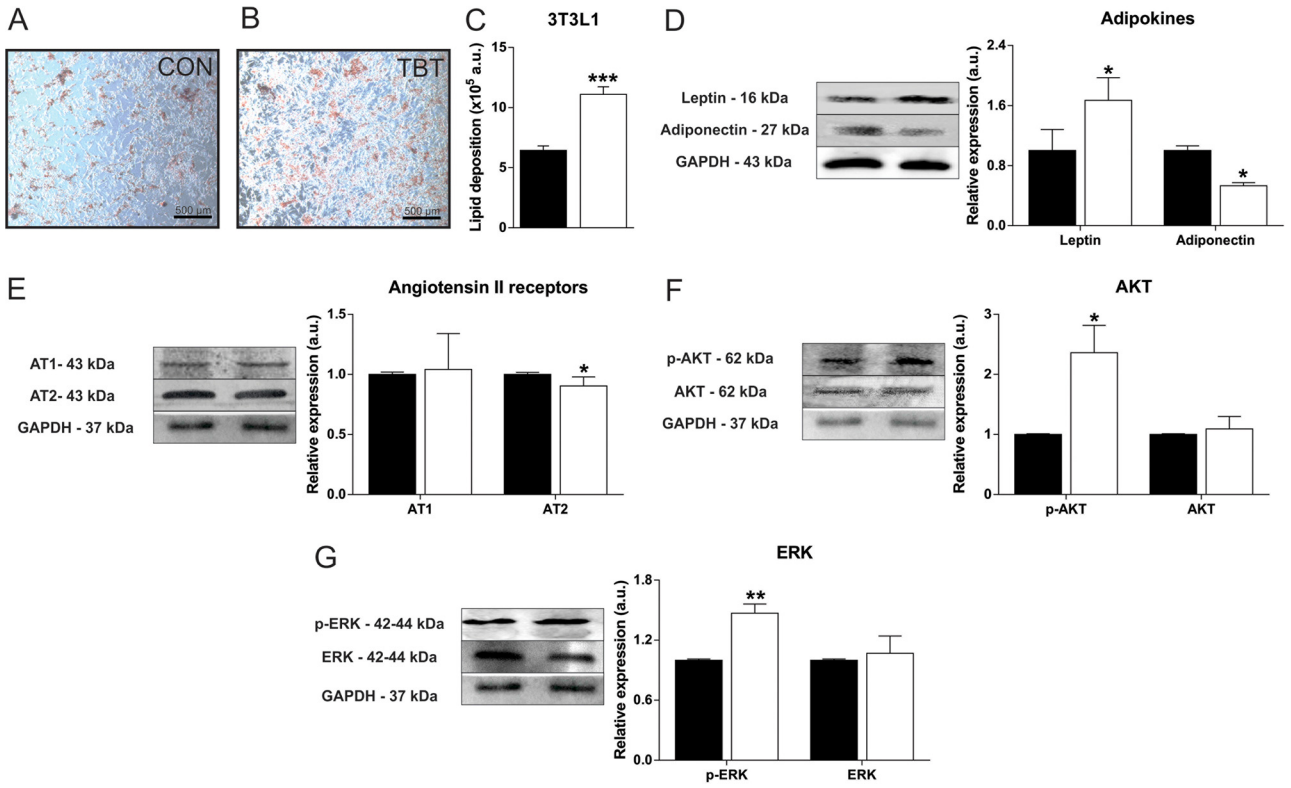

Fig. 4. 3T3L-1 exposed to TBT showed adipogenesis, adipokines expression alteration, AT2 down-expression and disrupted RAS pathway. (A–B), Oil-red stained photomicrography of 3T3L-1 CON and TBT exposed confirms the (C) Increased lipid deposition in 3T3L-1 TBT-exposed (n = 6). (D) The TBT exposure reflects in an Adipokines, increased leptin and reduced adiponectin, protein expression (n = 3). (E) Angiotensin II receptors (AT1R and AT2R) protein expression, reduced AT2R expression in TBT rats (n = 3). (F) increased p-AKT/AKT ratio and total AKT protein expression in WAT from TBT rats (n = 3). (G) increased p-ERK/ERK ratio and total ERK protein expression in WAT from TBT rats (n = 3). All data is expressed as the mean ± SEM. Student's t-test. * $p < 0.05$, ** $p < 0.01$, *** $p < 0.001$. Bar = 500 µm.

adiponectin protein expression, and increased leptin, AKT and ERK protein expression were observed in 3T3L1 cells exposed to TBT.

TBT effects correlate with adverse metabolism effects, and the induced obesity model is well established (Chamorro-Garcia et al., 2017). Our previous studies reported that 100 ng/kg/day TBT for 15 days increases body weight/adiposity and induces insulin resistance (IR), hyperinsulinemia, hyperleptinemia, and hypoadiponectinemia in female rats (Bertuloso et al., 2015; Sena et al., 2017). Our results are consistent with these previous findings, which demonstrated abnormal metabolic features in the TBT rats. We observed that in addition to obesity and IR, TBT also contributes to dyslipidemia with increased serum cholesterol, triglycerides (TG), and serum LDL levels and reduced HDL serum levels in female rats.

MetS is a clustering of risk factors characterized by the simultaneous occurrence of at least three of the following abnormal conditions: obesity, hyperglycemia, hypertension or dyslipidemia (Day, 2007; Wong et al., 2016). A general consensus exists regarding the main MetS components, but different definitions require different cutoff points and have different mandatory inclusion criteria. Although IR is considered a major pathological influence, only the World Health Organization (WHO) and European Group for the study of IR (EGIR) definitions include it among diagnostic criteria. Moreover, only the International Diabetes Federation (IDF) and National Cholesterol Education Program—Third Adult Treatment Panel (NCEP ATP III) definition includes waist circumference as an important component (Day, 2007; WHO - World and Health Organization, 2016). NCEP ATP III guidelines suggested that MetS is diagnosed when a person has three or more of five components, such as central obesity, increased TG levels, reduced HDL levels, hypertension and hyperglycemia (Alberti et al., 2006). MetS is inducible in different rodent models using specific diets. The use of a single type of diet (high-carbohydrate and fat) or a diet combination for 3–48 weeks induces different features of obesity, hyperglycemia, hypertension and dyslipidemia (Wong et al., 2016; Zhou et al., 2014). Thus, TBT stimulates obesity, IR, dyslipidemia (high TG and low HDL levels), *i.e.*, four out of five MetS diagnostic criteria defined by WHO and three out of five defined by NCEP ATPIII. Therefore, TBT acts as an inducer of MetS in our model.

Obesity is an abnormal fat condition that is typically accompanied by WAT expansion, low-grade inflammation, and an abnormal adipokine profile, which play an important role in metabolic disturbances, such as IR (Leal and Mafra, 2013; Mirzaei et al., 2013). Bertuloso et al. (2015) reported that TBT leads to obesity, abnormal adipocyte expansion, and inflammation with a high presence of mast cells. TBT promotes hyperleptinemia and hypoadiponectinemia in female rats (Sena et al., 2017). Our results are consistent with these previous findings, which demonstrated abnormal adipocyte hypertrophy, inflammation and serum adipokines in TBT rats.

OTs induce neuroinflammation by irregular gene expression control and cytokine secretion (Kraft et al., 2016; Lee et al., 2016). In addition, we revealed an important association among irregular transcript factor expression, adipokines levels, low-grade inflammation state and pro-inflammatory cytokines in obesity (Bernlohr et al., 2002; Febbraio, 2014). However, few studies evaluated the consequence of OT exposure, WAT adipokine profile and obesity (Ravanan et al., 2011). Thus, WAT nuclear factor-κB (NF-κB) and adipokine profiles in response to TBT exposure were assessed. Regarding NF-κB, we observed an increase in p50 and p65 subunit protein expression and decreased IκB subunit protein expression in WAT-TBT rats. The NF-κB is a family of transcription factor proteins that coordinates the expression of different genes that control immune responses. NF-κB subunit proteins (p65 and

p50) are present in the cytoplasm in association with the inhibitory protein that is known as an inhibitor of κB (IκB) (Li and Verma, 2002). Mitra et al. (2013) reported that high NF-κB protein expression (p65) was associated with neuronal inflammation of rat brain exposed to TBT (10–30 mg/kg) for 7 days (Mitra et al., 2013). Obesity activates NF-κB signaling and reduces IκB expression *via* low-grade inflammation (Catrysse and van Loo, 2017; Engin, 2017; Yan et al., 2014). Studies using mice lacking the p50 subunit of NF-κB exhibit protection against obesity and WAT accumulation/inflammation, supporting the notion that NF-κB is an important regulator of WAT metabolism (Minegishi et al., 2015).

Additionally, we observed high TNF-α and IL-6 levels and low IL-13 and IL-4 levels in WAT-TBT rats. Similarly, Ravanan et al (2011) reported high TNF-α and IL-6 expression in adipocytes/macrophages with altered leptin levels *in vitro* and abnormal WAT-TNF-α and adiponectin levels in ob/ob mice after trimethyltin exposure. TNF-α interferes negatively with insulin metabolism, resulting in hyperglycemia (Febbraio, 2014). In fact, obesity correlates with imbalances in interleukins, such as IL-4, IL-6, and IL-13, which either positively or negatively regulate systemic glucose/lipid metabolism (Cao, 2014; Febbraio, 2014). IL-4 and IL-13 also play important roles as anti-inflammatory cytokines and maintaining glucose homeostasis during obesity (Ouchi et al., 2011). Interactions between immune and metabolic cells exist in all major metabolic tissues, indicating that metabolic inflammation is a universal feature and a pathological basis for obesity-induced metabolic dysfunction (Eckel et al., 2005). Thus, the abnormalities in NFκB, TNF-α, IL-6, IL-4, and IL-13 in WAT reinforce the low-grade inflammation state, which is a typical MetS profile as reported in our current study after TBT exposure.

Recent studies reported that RAS components are expressed and play an important role in adipocyte function, such as adipogenesis and glucose/lipid signaling (Forrester et al., 2018; Slamkova et al., 2016). In obesity, other metabolic complications activate the synthesis of WAT-RAS components and/or induce irregular responsiveness to Ang II peptides that mediate MetS-specific disorders, such as abnormal WAT adipokine release and inflammation (Bruce and de Kloet, 2017; Putnam et al., 2012). Ang II is a principal active RAS peptide, playing different metabolic roles upon binding to WAT Ang-II receptors (AT1R and AT2R) that are G-protein-coupled receptors (De Kloet et al., 2010). In addition, WAT-RAS metabolic modulation results from other Ang-II peptide/receptor actions, such as Ang (1–7) (De Kloet et al., 2010). Thus, Ang-II modulates various pathways, such as NFκB, PPARγ, JAK/STAT, MAPK or ERK signaling cascades, which may culminate in IR and/or type 2 diabetes (Frigolet et al., 2013; De Kloet et al., 2010). Furthermore, several of these same pathways are also involved in the actions of various cytokines and/or other metabolic hormones, such as insulin.

Ang II infusion into human WAT reduced glucose uptake by AT1R (Boschmann et al., 2001; Kouyama et al., 2005). IR is improved by AT1R action reduction in obese Zucker rats (Henriksen et al., 2001). Our results are consistent with these previous findings, which revealed increased WAT-AT1R protein expression that could be associated with an IR observed in the TBT rats. Although AKT plays an important role in insulin signaling to stimulate glucose uptake in adipocytes (Cao, 2014), no significant change in pAKT/AKT and increased total AKT protein levels were observed in WAT-TBT rats. Reduced Ang (1–7) protein expression was also observed in WAT-TBT rats. Muñoz et al. (2010) reported that Ang (1–7) induces AKT phosphorylation in rat WAT (Muñoz et al., 2010). Ang II binding to AT1R alters pro-inflammatory adipokine secretion by TNF-α, ERK and p38 signaling, and reduced AT1R action improves adiponectin production in obese mouse WAT (Asamizu et al., 2009; Kurata et al., 2006). Ang II promotes leptin production in human adipocytes in an AT1R- and ERK 1/2-dependent manner (Skurk et al., 2005). Our results are consistent with these previous findings, which demonstrated that increased total ERK protein in WAT could be associated with increased leptin and reduced adiponectin levels in TBT rats. We also observed a reduction in p-p38/p38 total p38 protein expression in WAT-TBT rats. Ang II also influences lipid metabolism/lipogenesis, which is the production of fatty acids and its esterification into TG (Giani et al., 2012). Ang II increases FAS expression and TG accumulation in adipocytes (Ailhaud et al., 2002; Jones et al., 1997). Our results are consistent with these previous findings, which demonstrated increased WAT-FAS protein expression in TBT rats. PPARγ is a master regulator of adipocyte differentiation (Tontonoz et al., 1994). TBT promotes adipogenesis/lipogenesis and perturbs key regulators of metabolic pathways by altering RXR/PPARγ activation (Grün et al., 2006; Penza et al., 2011). Indeed, the association between PPARγ and RAS components was previously described (Tsai et al., 2004). Similar to findings of Bertuloso et al. (2015), we observed increased WAT PPARγ protein expression in TBT rats.

Despite a review reported by Yvan-Charvet and Quignard-Boulangé (2011) that reveals that both Ang II receptors may modulate fat mass expansion by WAT lipogenesis (AT2R) and lipolysis (AT1R), conflicting data exist about the role of Ang II and their receptors in adipocyte function. Mice lacking AT1R were protected from diet-induced obesity, revealing a synergistic contribution of AT1R and AT2R in mediating the effect of Ang II on WAT development (Kouyama et al., 2005). In contrast to AT1R, AT2R and Mas receptor knockout mice exhibited increased fat mass associated with higher WAT angiotensinogen expression, thereby suggesting a tight regulation of WAT Ang II production by Ang (1–7) (Santos et al., 2008). Recently, studies using knockout mice that block Ang II production prevented fat mass enlargement (Jayasooriya et al., 2008; Ohtaki et al., 2007). Similar findings were observed with RAS blockade (de Kloet et al., 2009). Further studies should help clarify whether Ang II modulates the NF-kB pathway, other adipokine pathways directly mediated by AT1R/AT2R and other Ang II peptide/receptor signaling pathways. Alternatively, Ang II could act through enhanced Toll-like receptor signaling secondary (Hwang, 2001). Thus, TBT leads to different RAS activities in WAT-TBT rats by disrupting AT1R/AT2R and Ang (1–7) signaling to control IR, adipogenesis, lipogenesis, and dyslipidemia at least in part by abnormal local inflammation.

On the other hand, when the *in vitro* TBT assay was evaluated, the model was confirmed with Oil red O staining, and the findings are consistent with the literature (Bertuloso et al., 2015). Summarizing our *in vivo* data, TBT stimulates adipocyte differentiation, induces leptin production and inhibits adiponectin secretion. In addition, in contrast to *in vivo* results, TBT treatment in 3T3L1 cells reduced AT2R levels, increased leptin expression, and reduced adiponectin protein expression. Mitchell et al. (1997) reported that adipocytes differentiation and lipid accumulation are associated with leptin production/release. We observed high lipid accumulation and high leptin expression in 3T3L1 cells after TBT exposure. Consistent with our data, Clasen et al. (2005) reported that blockade of AT2R leads to the inhibition of Ang II-induced adiponectin expression in 3T3L1 cells. Similarly, Ang II promotes leptin production in human fat cells *in vitro via* an ERK-dependent pathway (Skurk et al., 2005). Furthermore, we reported pERK/ERK and pAKT/AKT in 3T3L1 cells exposed to TBT, suggesting the relationship between leptin and adiponectin previously reported above (Asamizu et al., 2009; Kurata et al., 2006; Skurk et al., 2005). Thus, TBT promotes different RAS activities *in vitro*, disrupting AT1R/AT2R signaling to control adipogenesis/lipogenesis and glucose uptake at least in part *via* abnormal adipokine expression.

Based on data reported in this study, we hypothesize that the mechanism is TBT-exposure dependent (Fig. 5). We believe that TBT interferes with RAS components, stimulating AT1R upregulation. This overexpression leads to NF-κB pathway induction, which induces an inflammatory process (including inflammatory cell recruitment). AT1R promotes ERK 1/2 and p38 activation, resulting in high leptin and low AT2R levels that could reduce adiponectin production *in vitro*. FAS was augmented in TBT rats. Finally, Ang (1–7) downregulation is associated with dyslipidemia, WAT expansion, and AT1R activation, which results

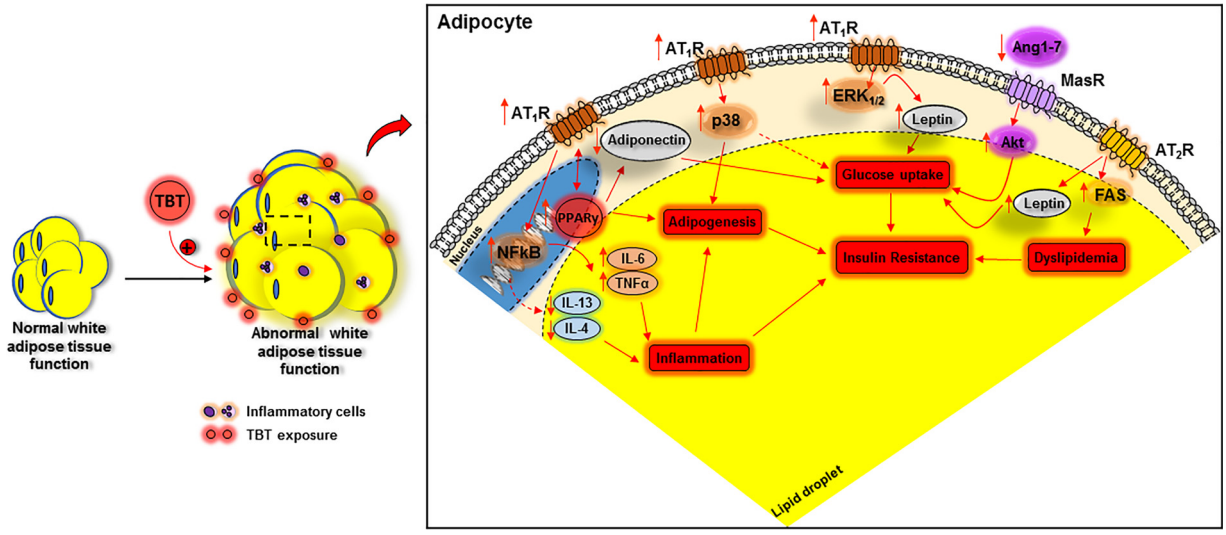

Fig. 5. Summary of TBT exposure effects in WAT. TBT exposure alters the RAS components in WAT, leading to an overexpression of AT1R, and Ang (1–7) reduction. AT1R overexpression is associated with an increase NFκB expression, which stimulates the pro-inflammatory cascade, IL-6 and TNFα, and inhibits the ant-inflammatory cytokines, IL-13 and IL-4. The pro-inflammatory cascade activation leads to a low-grade inflammation state, which is associated with increased adipogenesis. The elevated p38 expression, the increased of ERK 1/2 and hyperleptinemia and hypoadiponectinemia are linked to impaired glucose uptake, which also contributes to adipogenesis. Also, the glucose uptake could be associated wih Akt expression. The FAS Overexpression in WAT is associated with dyslipidemia after TBT exposure. In conclusion, we could observe that TBT exposure induced an inflammatory process leading adipogenesis, insulin resistance and dyslipidemia, associated with metabolic syndrome features.

in a commitment glucose uptake. Furthermore, PPARγ cross-talk to both Ang II receptors and Ang (1–7) interferes with all downstream cascades (Zhang et al., 2013). In addition, the adverse effects of TBT are generally dependent on PPARγ. Thus, PPARγ *per se* participates in the development of adipogenesis and obesity. Therefore, these findings help us to clarify the potential side effects of TBT on metabolism.

In conclusion, the present study demonstrates that TBT is involved in the constellation of factors that contribute to MetS development. We believe that this development is partly mediated by WAT-RAS components, representing a new alternative pathway that TBT targets to interfere with physiological metabolism. Thus, this discovery could be an important method to offer treatments for this pollutant, and increased public awareness of the risks of these EDCs risks and their use in routine life is warranted.

Conflict of interest

The authors declare that the research was conducted in the absence of any commercial or financial relationships that could be construed as a potential conflict of interest.

Transparency document

The Transparency document associated with this article can be found in the online version.

Acknowledgements

LCFL and JBG are supported by the State Agency for the Development of Science and Technology (FAPES, # 72630477 - T.O. 965/15; and FAPES T.O. # 179/2017, CNPq #304724/2017-3/ Nº 12/2017, respectively). The histology was performed at the facilities of the Multiuser Laboratory of Molecular Histology and Immunohistochemistry/UFES.

Appendix A. Supplementary data

Supplementary material related to this article can be found, in the online version, at doi:https://doi.org/10.1016/j.toxlet.2018.08.018.

References

Ailhaud, G., Teboul, M., Massiera, F., 2002. Angiotensinogen, adipocyte differentiation and fat mass enlargement. Curr. Opin. Clin. Nutr. Metab. Care 5, 385–389.

Alberti, G., Zimmet, P., Grundy, S.M., 2006. The IDF Consensus Worldwide Definition of the Metabolic Syndrome. International Diabetes Federation, Brussels. https://doi.org/10.2337/diacare.24.4.683.

Araújo, Fa, Rocha, Ma, Mendes, J.B., Andrade, S.P., 2010. Atorvastatin inhibits inflammatory angiogenesis in mice through down regulation of VEGF, TNF-alpha and TGF-beta1. Biomed. Pharmacother. 64, 29–34. https://doi.org/10.1016/j.biopha.2009.03.003.

Asamizu, S., Urakaze, M., Kobashi, C., Ishiki, M., Norel Din, A.K., Fujisaka, S., Kanatani, Y., Bukahari, A., Senda, S., Suzuki, H., Yamazaki, Y., Iwata, M., Usui, I., Yamazaki, K., Ogawa, H., Kobayashi, M., Tobe, K., 2009. Angiotensin II enhances the increase in monocyte chemoattractant protein-1 production induced by tumor necrosis factor-from 3T3-L1 preadipocytes. J. Endocrinol. 202, 199–205. https://doi.org/10.1677/JOE-08-0363.

Barcelos, L., Talvani, A., Vieira, L., Cassali, G., Andrade, S., Teixeira, M.M., 2005. Impaired inflammatory angiogenesis, but not leukocyte influx, in mice lacking TNFR1. J. Leukoc. Biol. 78, 352–358. https://doi.org/10.1189/jlb.1104682.0741-5400/05/0078-352.

Bergman, Å., Heindel, J., Jobling, S., Kidd, K., Zoeller, R.T., 2012. State-of-the-science of endocrine disrupting chemicals, 2012. Toxicol. Lett. 211, S3. https://doi.org/10.1016/j.toxlet.2012.03.020.

Bernlohr, D.A., Jenkins, A.E., Bennaars, A.A., 2002. In: Vence, J.E., Vence, D. (Eds.), Adipose Tissue and Lipid Metabolism. Biochem. Lipids, Lipoproteins Membr, 4th ed. Elsevier Sci, Amsterdam, pp. 263–289.

Bertuloso, B.D., Podratz, P.L., Merlo, E., de Araújo, J.F.P., Lima, L.C.F., de Miguel, E.C., de Souza, L.N., Gava, A.L., de Oliveira, M., Miranda-Alves, L., Carneiro, M.T.W.D., Nogueira, C.R., Graceli, J.B., 2015. Tributyltin chloride leads to adiposity and impairs metabolic functions in the rat liver and pancreas. Toxicol. Lett. 235, 45–59. https://doi.org/10.1016/j.toxlet.2015.03.009.

Boschmann, M., Ringel, J., Klaus, S., Sharma, A.M., 2001. Metabolic and hemodynamic response of adipose tissue to angiotensin II. Obes. Res. 9, 486–491. https://doi.org/10.1038/oby.2001.63.

Bruce, E.B., de Kloet, A.D., 2017. The intricacies of the renin-angiotensin-system in metabolic regulation. Physiol. Behav. 178, 157–165. https://doi.org/10.1016/j.physbeh.2016.11.020.

Cairelli, M.J., Miller, C.M., Fiszman, M., Workman, T.E., Rindflesch, T.C., 2013. Semantic MEDLINE for discovery browsing: using semantic predications and the literature-based discovery paradigm to elucidate a mechanism for the obesity paradox. AMIA … Annu. Symp. Proceedings. AMIA Symp. 2013, 164–173.

Canesso, M., Vieira, A., Castro, T., Schirmer, B., Martins, F., Rachid, M., Nicoli, J., Teixeira, M., Barcelos, L., 2014. Skin Wound Healing is accelerated and scarless in the absence of commensal microbiota. J. Immunol. 193, 5171–5180.

Cao, H., 2014. Adipocytokines in obesity and metabolic disease. J. Endocrinol. 220, T47–T59. https://doi.org/10.1530/JOE-13-0339.

Catrysse, L., van Loo, G., 2017. Inflammation and the metabolic syndrome: the tissue-specific functions of NF-κB. Trends Cell Biol. 27, 417–429. https://doi.org/10.1016/j.tcb.2017.01.006.

Chamorro-Garcia, R., Diaz-Castillo, C., Shoucri, B.M., Käch, H., Leavitt, R., Shioda, T., Blumberg, B., 2017. Ancestral perinatal obesogen exposure results in a transgenerational thrifty phenotype in mice. Nat. Commun. 8, 2012. https://doi.org/10.1038/s41467-017-01944-z.

Clasen, R., Schupp, M., Foryst-Ludwig, A., Sprang, C., Clemenz, M., Krikov, M., Thöne-Reineke, C., Unger, T., Kintscher, U., 2005. PPARgamma-activating angiotensin type-1 receptor blockers induce adiponectin. Hypertension 46 (1), 137–143.

Day, C., 2007. Metabolic syndrome, or what you will: definitions and epidemiology. Diabetes Vasc. Dis. Res. 4, 32–38. https://doi.org/10.3132/dvdr.2007.003.

de Kloet, A.D., Krause, E.G., Kim, D.-H., Sakai, R.R., Seeley, R.J., Woods, S.C., 2009. The effect of angiotensin-converting enzyme inhibition using captopril on energy balance and glucose homeostasis. Endocrinology 150, 4114–4123. https://doi.org/10.1210/en.2009-0065.

De Kloet, A.D., Krause, E.G., Woods, S.C., 2010. The renin angiotensin system and the metabolic syndrome. Physiol. Behav. 100, 525–534. https://doi.org/10.1016/j.physbeh.2010.03.018.The.

De Picoli Souza, K., Da Silva, E.D., Batista, E.C., Reis, F.C.G., Silva, S.M.A., Castro, C.H.M., Luz, J., Pesquero, J.L., Dos Santos, E.L., Pesquero, J.B., 2015. Early pharmacological inhibition of angiotensin-I converting enzyme activity induces obesity in adulthood. Front. Pharmacol. 6, 1–10. https://doi.org/10.3389/fphar.2015.00075.

Eckel, R.H., Alberti, K.G.M.M., Grundy, S.M., Zimmet, P.Z., 2005. The metabolic syndrome. Lancet 365, 1415–1428. https://doi.org/10.1016/S0140-6736(09)61794-3.

Endlich, P.W., Claudio, E.R., Lima, L.C. F, R.J.R. Peluso, A.A. Stefanon, I. Bissoli, N.S. Lemos, V.S. Santos, R.A. Abreu, G.R., 2017. Exercise modulates the aortic renin-angiotensin system independently of estrogen therapy in ovariectomized hypertensive rats. https://doi.org/10.1016/j.peptides.2016.11.010.

Engin, A.B., 2017. MicroRNA and Adipogenesis. pp. 489–509.. https://doi.org/10.1007/978-3-319-48382-5_21.

Febbraio, M.A., 2014. Role of interleukins in obesity: implications for metabolic disease. Trends Endocrinol. Metab. 25, 312–319. https://doi.org/10.1016/j.tem.2014.02.004.

Forrester, S.J., Booz, G.W., Sigmund, C.D., Coffman, T.M., Kawai, T., Rizzo, V., Scalia, R., Eguchi, S., 2018. Angiotensin II signal transduction: an update on mechanisms of physiology and pathophysiology. Physiol. Rev. 98, 1627–1738. https://doi.org/10.1152/physrev.00038.2017.

Frigolet, M.E., Torres, N., Tovar, A.R., 2013. The renin–angiotensin system in adipose tissue and its metabolic consequences during obesity. J. Nutr. Biochem. 24, 2003–2015. https://doi.org/10.1016/j.jnutbio.2013.07.002.

Fujimoto, T., Parton, R.G., 2011. Not just fat: the structure and function of the lipid droplet. Cold Spring Harb. Perspect. Biol. 3https://doi.org/10.1101/cshperspect.a004838. a004838–a004838.

Giani, J.F., Burghi, V., Veiras, L.C., Tomat, A., Muñoz, M.C., Cao, G., Turyn, D., Toblli, J.E., Dominici, F.P., 2012. Angiotensin-(1-7) attenuates diabetic nephropathy in Zucker diabetic fatty rats. Am. J. Physiol. Renal Physiol. 302, F1606–F1615. https://doi.org/10.1152/ajprenal.00063.2012.

Grün, F., Blumberg, B., 2006. Environmental obesogens: organotins and endocrine disruption via nuclear receptor signaling. Endocrinology 147, S50–5. https://doi.org/10.1210/en.2005-1129.

Grün, F., Watanabe, H., Zamanian, Z., Maeda, L., Arima, K., Cubacha, R., Gardiner, D.M., Kanno, J., Iguchi, T., Blumberg, B., 2006. Endocrine-disrupting organotin compounds are potent inducers of Adipogenesis in vertebrates. Mol. Endocrinol. 20, 2141–2155. https://doi.org/10.1210/me.2005-0367.

Henriksen, E.J., Jacob, S., Kinnick, T.R., Teachey, M.K., Krekler, M., 2001. Selective angiotensin II receptor antagonism reduces insulin resistance in obese Zucker rats. Hypertens. (Dallas, Tex. 1979) 38, 884–890.

Hwang, D., 2001. Modulation of the expression of cyclooxygenase-2 by fatty acids mediated through Toll-like receptor 4-derived signaling pathways. FASEB J. 15, 2556–2564. https://doi.org/10.1096/fj.01-0432com.

Jayasooriya, A.P., Mathai, M.L., Walker, L.L., Begg, D.P., Denton, D.A., Cameron-Smith, D., Egan, G.F., McKinley, M.J., Rodger, P.D., Sinclair, A.J., Wark, J.D., Weisinger, H.S., Jois, M., Weisinger, R.S., 2008. Mice lacking angiotensin-converting enzyme have increased energy expenditure, with reduced fat mass and improved glucose clearance. Proc. Natl. Acad. Sci. 105, 6531–6536. https://doi.org/10.1073/pnas.0802690105.

Jones, B.H., Standridge, M.K., Moustaid, N., 1997. Angiotensin II increases lipogenesis in 3T3-L1 and human adipose cells 1. Endocrinology 138, 1512–1519. https://doi.org/10.1210/endo.138.4.5038.

Kelly, T., Yang, W., Chen, C.-S., Reynolds, K., He, J., 2008. Global burden of obesity in 2005 and projections to 2030. Int. J. Obes. (Lond.) 32, 1431–1437. https://doi.org/10.1038/ijo.2008.102.

Kouyama, R., Suganami, T., Nishida, J., Tanaka, M., Toyoda, T., Kiso, M., Chiwata, T., Miyamoto, Y., Yoshimasa, Y., Fukamizu, A., Horiuchi, M., Hirata, Y., Ogawa, Y., 2005. Attenuation of diet-induced weight gain and adiposity through increased energy expenditure in mice lacking angiotensin II type 1a receptor. Endocrinology 146, 3481–3489. https://doi.org/10.1210/en.2005-0003.

Kraft, A.D., McPherson, C.A., Harry, G.J., 2016. Association between microglia, inflammatory factors, and complement with loss of Hippocampal Mossy Fiber Synapses induced by Trimethyltin. Neurotox. Res. 30, 53–66. https://doi.org/10.1007/s12640-016-9606-8.

Kurata, A., Nishizawa, H., Kihara, S., Maeda, N., Sonoda, M., Okada, T., Ohashi, K., Hibuse, T., Fujita, K., Yasui, A., Hiuge, A., Kumada, M., Kuriyama, H., Shimomura, I., Funahashi, T., 2006. Blockade of Angiotensin II type-1 receptor reduces oxidative stress in adipose tissue and ameliorates adipocytokine dysregulation. Kidney Int. 70, 1717–1724. https://doi.org/10.1038/sj.ki.5001810.

Leal, V. de O., Mafra, D., 2013. Adipokines in obesity. Clin. Chim. Acta 419, 87–94. https://doi.org/10.1016/j.cca.2013.02.003.

Lee, S., Yang, M., Kim, J., Kang, S., Kim, J., Kim, J.C., Jung, C., Shin, T., Kim, S.-H., Moon, C., 2016. Trimethyltin-induced hippocampal neurodegeneration: amechanism-based review. Brain Res. Bull. 125, 187–199. https://doi.org/10.1016/j.brainresbull.2016.07.010.

Li, Q., Verma, I.M., 2002. NF-κB regulation in the immune system. Nat. Rev. Immunol. 2, 725–734. https://doi.org/10.1038/nri910.

Lima, L.C., Porto, M.L., Campagnaro, B.P., Tonini, C.L., Nogueira, B.V., Pereira, T.M., Vasquez, E.C., Meyrelles, S.S., 2012. Mononuclear Cell Therapy Reverts Cuff-induced Thrombosis in Apolipoprotein E-deficient Mice. https://doi.org/10.1186/1476-511X-11-96.

Lima, L.C.F., Saliba, S.W., Andrade, J.M.O., Cunha, M.L., Cassini-Vieira, P., Feltenberger, J.D., Barcelos, L.S., Guimarães, A.L.S., De-Paula, A.M.B., de Oliveira, A.C.P., Santos, S.H.S., 2016. Neurodegeneration Alters Metabolic Profile and Sirt 1 signaling in high-fat-induced obese mice. Mol. Neurobiol. 1–11. https://doi.org/10.1007/s12035-016-9927-x.

Ludgero-Correia, A., Aguila, M.B., Mandarim-de-Lacerda, C.A., Faria, T.S., 2012. Effects of high-fat diet on plasma lipids, adiposity, and inflammatory markers in ovariectomized C57BL/6 mice. Nutrition 28, 316–323. https://doi.org/10.1016/j.nut.2011.07.014.

Minegishi, Y., Haramizu, S., Misawa, K., Shimotoyodome, A., Hase, T., Murase, T., 2015. Deletion of nuclear factor-κB p50 upregulates fatty acid utilization and contributes to an anti-obesity and high-endurance phenotype in mice. Am. J. Physiol. Metab. 309, E523–E533. https://doi.org/10.1152/ajpendo.00071.2015.

Mirzaei, K., Hossein-nezhad, A., Keshavarz, S., Koohdani, F., Saboor-Yaraghi, A.A., Hosseini, S., Eshraghian, M.R., Djalali, M., 2013. Crosstalk between circulating peroxisome proliferator-activated receptor gamma, adipokines and metabolic syndrome in obese subjects. Diabetol. Metab. Syndr. 5, 79. https://doi.org/10.1186/1758-5996-5-79.

Mitchell, S.E., Rees, W.D., Hardie, L.J., Hoggard, N., Tadayyon, M., Arch, J.R., Trayhurn, P., 1997. ob gene expression and secretion of leptin following differentiation of rat preadipocytes to adipocytes in primary culture. Biochem. Biophys. Res. Commun. 230 (2), 360–364.

Mitra, S., Gera, R., Siddiqui, W.A., Khandelwal, S., 2013. Tributyltin induces oxidative damage, inflammation and apoptosis via disturbance in blood-brain barrier and metal homeostasis in cerebral cortex of rat brain: an in vivo and in vitro study. Toxicology 310, 39–52. https://doi.org/10.1016/j.tox.2013.05.011.

Muñoz, M.C., Giani, J.F., Dominici, F.P., 2010. Angiotensin-(1-7) stimulates the phosphorylation of Akt in rat extracardiac tissues in vivo via receptor Mas. Regul. Pept. 161, 1–7. https://doi.org/10.1016/j.regpep.2010.02.001.

National Research Council (US) Committee to Review EPA's Toxicological Assessment of Tetrachloroethylene, 2010. Review of the Environmental Protection Agency's Draft IRIS Assessment of Tetrachloroethylene.

Ohtaki, K., Aihara, M., Takahashi, H., Fujita, H., Takahashi, K., Funabashi, T., Hirasawa, T., Ikezawa, Z., 2007. Effects of tributyltin on the emotional behavior of C57BL/6 mice and the development of atopic dermatitis-like lesions in DS-Nh mice. J. Dermatol. Sci. 47, 209–216. https://doi.org/10.1016/j.jdermsci.2007.05.001.

Ouchi, N., Parker, J.L., Lugus, J.J., Walsh, K., 2011. Adipokines in inflammation and metabolic disease. Nat. Rev. Immunol. 11, 85–97. https://doi.org/10.1038/nri2921.

Penza, M., Jeremic, M., Marrazzo, E., Maggi, A., Ciana, P., Rando, G., Grigolato, P.G., Di Lorenzo, D., 2011. The environmental chemical tributyltin chloride (TBT) shows both estrogenic and adipogenic activities in mice which might depend on the exposure dose. Toxicol. Appl. Pharmacol. 255, 65–75. https://doi.org/10.1016/j.taap.2011.05.017.

Pereira, S.S., Teixeira, L.G., Aguilar, E.C., Matoso, R.O., Soares, F.L.P., Ferreira, A.V.M., Alvarez-Leite, J.I., 2012. Differences in adipose tissue inflammation and oxidative status in C57BL/6 and ApoE-/- mice fed high fat diet. Anim. Sci. J. 83, 549–555. https://doi.org/10.1111/j.1740-0929.2011.00982.x.

Putnam, K., Shoemaker, R., Yiannikouris, F., Cassis, L.A., 2012. The renin-angiotensin system: a target of and contributor to dyslipidemias, altered glucose homeostasis, and hypertension of the metabolic syndrome. Am. J. Physiol. Circ. Physiol. 302, H1219–H1230. https://doi.org/10.1152/ajpheart.00796.2011.

Ravanan, P., Harry, G.J., Awada, R., Hoareau, L., Tallet, F., Roche, R., Lefebvre d'Hellencourt, C., 2011. Exposure to an organometal compound stimulates adipokine and cytokine expression in white adipose tissue. Cytokine 53, 355–362. https://doi.org/10.1016/j.cyto.2010.11.015.

Rubio-ruíz, M.E., Valle-mondragón, L., Del, Castrejón-tellez, V., Carreón-torres, E., 2014. Peptides angiotensin II and 1-7 during aging in metabolic syndrome rats. Expression of AT1, AT2 and Mas receptors in abdominal white adipose tissue. Peptides 57, 101–108. https://doi.org/10.1016/j.peptides.2014.04.021.

Santos, H.S., Fernandes, L.R., Mario, É.G., Ferreira, A.V.M., Pôrto, L.C.J., Alvarez-leite, J.I., Botion, L.M., Bader, M., Alenina, N., Santos, R.A.S., 2008. Mas deficiency in FVB/N mice produces marked changes in lipid and glycemic metabolism. Diabetes 57, 340–347. https://doi.org/10.2337/db07-0953.2DOG.

Sena, G.C., Freitas-Lima, L.C., Merlo, E., Podratz, P.L., de Ara?jo, J.F.P., Brand?o, P.A.A., Carneiro, M.T.W.D., Zicker, M.C., Ferreira, A.V.M., Takiya, C.M., de Lemos Barbosa, C.M., Morales, M.M., Santos-Silva, A.P., Miranda-Alves, L., Silva, I.V., Graceli, J.B., 2017. Environmental obesogen tributyltin chloride leads to abnormal hypothalamic-pituitary-gonadal axis function by disruption in kisspeptin/leptin signaling in female rats. Toxicol. Appl. Pharmacol. 319, 22–38. https://doi.org/10.1016/j.taap.2017.01.021.

Skurk, C., Maatz, H., Rocnik, E., Bialik, A., Force, T., Walsh, K., 2005. Glycogen-synthase Kinase3beta/beta-catenin axis promotes angiogenesis through activation of vascular endothelial growth factor signaling in endothelial cells. Circ. Res. 96, 308–318.

https://doi.org/10.1161/01.RES.0000156273.30274.f7.
Slamkova, M., Zorad, S., Krskova, K., 2016. Alternative renin-angiotensin system pathways in adipose tissue and their role in the pathogenesis of obesity. Endocr. Regul. 50, 229–240. https://doi.org/10.1515/enr-2016-0025.
Tontonoz, P., Hu, E., Spiegelman, B.M., 1994. Stimulation of adipogenesis in fibroblasts by PPARγ2, a lipid-activated transcription factor. Cell 79, 1147–1156. https://doi.org/10.1016/0092-8674(94)90006-X.
Tsai, Y.-S., Kim, H.-J., Takahashi, N., Kim, H.-S., Hagaman, J.R., Kim, J.K., Maeda, N., 2004. Hypertension and abnormal fat distribution but not insulin resistance in mice with P465L PPARgamma. J. Clin. Invest. 114, 240–249. https://doi.org/10.1172/JCI20964.
WHO - World and Health Organization, 2016. Obesity and Overweight: Fact Sheet N°311 [WWW Document]. URL. (Accessed June 17). http://www.who.int/mediacentre/factsheets/fs311/en/.
Wong, S.K., Chin, K.-Y., Suhaimi, F.H., Fairus, A., Ima-Nirwana, S., 2016. Animal models of metabolic syndrome: a review. Nutr. Metab. (Lond). 13 (65). https://doi.org/10.1186/s12986-016-0123-9.
Yan, J., Zhang, H., Yin, Y., Li, J., Tang, Y., Purkayastha, S., Li, L., Cai, D., 2014. Obesity- and aging-induced excess of central transforming growth factor-β potentiates diabetic development via an RNA stress response. Nat. Med. 20, 1001–1008. https://doi.org/10.1038/nm.3616.
Yvan-Charvet, L., Quignard-Boulangé, A., 2011. Role of adipose tissue renin-angiotensin system in metabolic and inflammatory diseases associated with obesity. Kidney Int. 79 (2), 162–168. https://doi.org/10.1038/ki.2010.391.
Zhang, X., Tan, F., Brovkovych, V., Zhang, Y., Lowry, J.L., Skidgel, R.A., 2013. Carboxypeptidase M augments kinin B1 receptor signaling by conformational cross-talk and enhances endothelial nitric oxide output. Biol. Chem. 394, 335–345. https://doi.org/10.1515/hsz-2012-0290.
Zhou, X., Han, D., Xu, R., Li, S., Wu, H., Qu, C., Wang, F., Wang, X., Zhao, Y., 2014. A model of metabolic syndrome and related diseases with intestinal endotoxemia in rats fed a high fat and high sucrose diet. PLoS One 9, e115148. https://doi.org/10.1371/journal.pone.0115148.